# Microalgae Cell Separation and Concentration in a Microfluidic Channel under the Dielectrophoretic (DEP) Effect

Arohi Barai[1*], Niklas Boldt[2], Mario Birkholz[1]
1. IHP – Leibniz-Institut für innovative Mikroelektronik, Im Technologiepark 25, 15236 Frankfurt (Oder), Germany
2. Fachgebiet Sensorik und Aktuatorik, Technische Universität Berlin, 10587 Berlin, Germany
*Corresponding author: barai@ihp-microelectronics.com

**Abstract:** Microalgae biomass is considered as a source of lipids in the production of pharmaceuticals, nutrients, and renewable biofuels. Dielectrophoresis (DEP) has evolved as an interesting technology allowing the vital, impeccable, and label-free cell sorting of microalgae in microfluidic systems. In this work, COMSOL Multiphysics 5.4 is used to find the electro-mechanical parameters to achieve efficient and flawless cell separation by DEP methods. The throughput to be obtained in microfluidic channels may be significantly increased by multiplying the number of deflector electrodes that act upon passing microalgae cells. According to our study, high separation efficiencies can be achieved, while the heating of the medium can be restricted to only a few °C.

**Keywords:** Microalgae, *C. reinhardtii*, cell separation, dielectrophoresis, laminar flow, simulation

## Introduction

Microalgae are mostly single-cell green algae that are widely found in soil and freshwater around the world. *Chlamydomonas reinhardtii*, for instance, is a model organism that is studied in the production of pharmaceuticals, biofuel, and hydrogen making [1]. Biofuel production requires effective and low-cost cell separation downstream processes where microalgae cells are concentrated and differentiated based on their lipid content [2].

Dielectrophoresis is a phenomenon in which dielectric particles are subjected to a force known as the dielectrophoretic(DEP) force by an oscillating non-uniform electric field [3]. This mechanism might be used in the implementation of microalgae cell separation (based on their lipid content) because of its efficient and label-free cell sorting process inside a microfluidic system equipped with electrically conducting electrodes at the sidewall of a microchannel (for instance sandwich structure in **Figure 1**)[4,5]. Practically, when microalgae cells are pumped into a microfluidic system and an AC voltage source is applied across the electrodes, it leads to the generation of a non-uniform electric field that interacts with the induced electrical dipole moment associated with the microalga [6]. When they move in line or towards the highest electric field, the phenomenon is known as positive DEP (pDEP) and when they move away from this highest electric field, it gives rise to negative DEP (nDEP)[7,8].

The nature, strength, and effect of DEP force on microalgae depend on the electrical parameters of the medium, and the microalgae like electrical permittivity ($\varepsilon$) and electrical conductivity ($\sigma$) [9,10]. In order to find a trade-off between them, COMSOL Multiphysics is used as a finite element simulation tool. The physics, study, equations used in the simulation are described in subsequent sections.

## Computational methods

**Geometry:** Two 3D model structures were created in COMSOL geometry for *microfluidic particle separation* (*MPS*) and other for *electro-thermal simulation* (*ETS*). In the *MPS* module, the microfluidic channel was realized with a geometry i.e. 5 mm long, 0.3 mm wide, and 0.05 mm high (**Figure 1**). Multiple electrode configurations were designed on the top and bottom of this microchannel as an array structure. Each array consisted of 4 electrodes with 14 arrays in total i.e. 56 electrode pairs on the top and bottom of the microchannel. This electrode geometry was designed to achieve high throughput in cell separation. In the microchannel, there were two pairs of inlets and outlets, which were used for injection and collection fluid and microalgae at the inlets and outlets respectively [11,12].

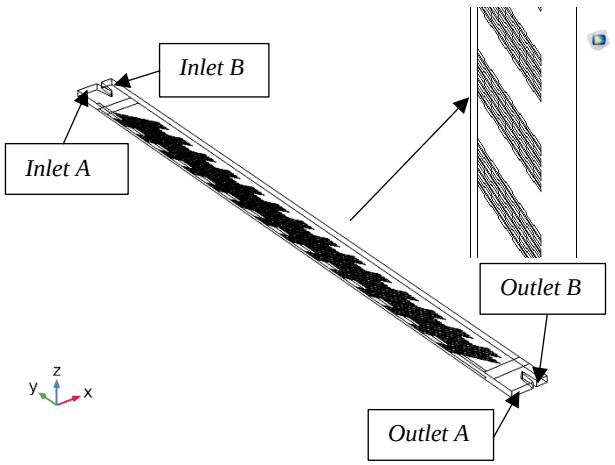


**Figure 1:** Microchannel geometry (0.3 mm wide (x-axis), 5 mm long (y-axis), and 0.05 mm high (z-axis)). There are 56 pairs of top and bottom electrodes as 14 pairs of arrays (each array has 4 electrodes). The electrodes (zoom version is shown on the top right) have an alternate width in between 10 µm and 20 µm with a skew-symmetric shape (as seen on top right corner). There are 2 inlets (A, B) and 2 outlets (A, B) in the microchannel.

The *ETS* geometry contained a microfluidic setup, where multiple microchannels parallel to each other were created as the physical gap between PDMS (polydimethylsiloxane) sheets (**Figure 2**). The entire setup was covered with silica glass substrate on top and bottom. However, the bottom silica glass substrate was plunged into a copper block (as a niche structure) which was used as a heat sink.

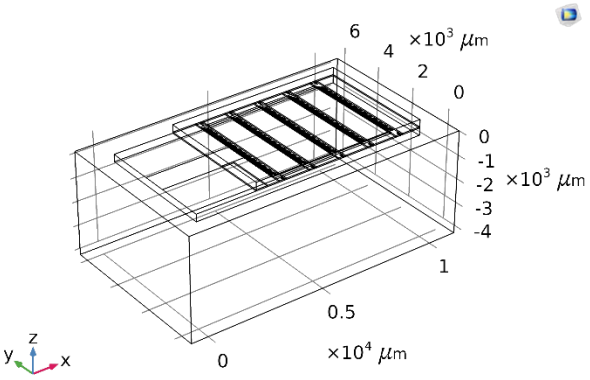


**Figure 2:** The microchannel setup (11.8 mm wide, 5 mm long, and 4.3 mm high). There are 5 microchannels that run parallel to each other which are created in between sheets of PDMS. The upper and lower substrates (300 µm high) exerts electric field in between the microchannel through the electrode array. There is a heat sink in the bottom where the bottom substrate is plunged as a niche structure.

**Simulation Setup:** There were two objectives of this simulation task. The first one was to find the right set of electro-mechanical parameters i.e. AC-DEP voltage, frequency of operation, and maximum fluid velocity of the medium at which the microalgae could be efficiently and flawlessly separated based on their lipid content through particle trajectories in the *MPS* module.

The other objective was to study the temperature distribution in the microfluidic setup (that contained the microchannel) due to the electric field generated by the electrodes. This simulation was realized in *ETS* module.

In the *MPS* module, two types/sizes of *C. reinhardtii* cells were suspended inside sweet water medium and set to pass through the microfluidic channel at different fluid velocity. The medium was subjected to different voltage amplitude at different frequency. Meanwhile, the *electrical current (ec)* physics module was used to impart AC-DEP voltage amplitude through electrodes.

The *laminar flow (spf)* physics module was used to create an uni-directional flow of the medium (containing microalgae) and buffer solution. Then, *particle tracing for fluid flow (fpt)* physics module was used in conjugation with drag and dielectric force to understand the dielectrophoresis inside the channel [7,11]. The simulation parameters of the microalgae and medium are defined underneath in **Table 1**.

**Table 1:** Physical parameters used in the simulation for the *C. reinhardtii* with low and high lipid contents along with water as medium.

| | |
|---|---|
| ***C. reinhardtii*: High lipid content** | |
| Density (kg/m$^3$) | 1000 |
| Elect. Conductivity (S/m) | 0.2 |
| Rel. permittivity | 60 |
| Cell diameter (µm) | 15 |
| ***C. reinhardtii*: Low lipid content** | |
| Density (kg/m$^3$) | 999 |
| Elect. Conductivity (S/m) | 1.2 |
| Rel. permittivity | 60 |
| Cell diameter (µm) | 14.5 |
| **Medium (water)** | |
| Density (kg/m$^3$) | 997 |
| Elect. Conductivity (mS/m) | 55 |
| Rel. permittivity | 80 |
| Dyn. viscosity (kg/s·m) | 0.001 |

In the *EPS* module, *electrical current (ec)* and *laminar flow (spf)* physics modules were used (as mentioned in the previous paragraph). However, an additional physics module i.e. *heat transfer in the fluid (ht)* along with Multiphysics module was used to understand the temperature distribution inside the microfluidic setup.

**Governing equations:** As per the condition of the two simulation process (as mentioned in the previous section), different governing equations were used to model the particle trajectories in *MPS* and *EPS* modules. The top electrodes on the microfluidic channels are connected to the *voltage source* and bottom electrodes are connected to *ground*. This electric potential ($V$) leads to an electric field ($E$), which is simulated by the *electric current (ec)* module. It is represented in *eq.(3)*. The static form of equation continuity is represented in *eq.(1-2)*, where $\sigma$ is the electrical conductivity of the electrode and $J_e$ is an externally generated current density.

$$\nabla \cdot J = Q_{j \cdot v} \quad (1)$$

$$J = \sigma E + J_e \quad (2)$$

$$E = -\nabla V \quad (3)$$

The medium used in this simulation was *water*, which is considered as an incompressible fluid because the change in pressure is too small to make a substantial change to its density. Its movement and velocity within the microchannel are governed by Navier-stokes equation. *Laminar flow (spf)* module was used in this simulation to study the flow of medium within the microchannel as seen underneath in *eq.(4-6)*.

Here $u$ denotes velocity vector, $\mu$ and $\rho$ represent the dynamic viscosity and density of the medium respectively. $K$ is the viscous force and $F$ signifies volume force vector acting on the fluid.

$$\rho(u \times \nabla)u = \nabla \cdot [-\rho l + K] + F \quad (4)$$

$$\rho \nabla \cdot (u) = 0 \quad (5)$$

$$K = \mu(\nabla u + (\nabla u)^T) = 0 \quad (6)$$

When the solution containing microalgae passes through the microfluidic channel under a non-uniform electric field, drag and DEP force play a key role in the nature of the flow. Their combined effect was observed in *particle tracing for fluid flow module (fpt).*

Drag force is a type of friction force acting opposite to the relative motion of an object moving with respect to a surrounding fluid [12]. It was calculated as per Stokes drags law as per *eq. (7-8*).

$$F_D = \frac{1}{\tau_p} m_p (u - v) \quad (7)$$

$$\tau_p = \frac{\rho_p d_p^2}{18\mu} \quad (8)$$

In the above two equations, $F_D$ denotes drag force, $\tau_p$ signifies velocity response of particles, $u$ and $v$ are the particle and fluid velocity respectively. Particle mass is represented by $m_p$. Particle density and diameter are denoted by $\rho_p$ and $d_p$ respectively. In order to trap, attract or repel the microalgae, DEP force was required. As per the setup, the microalgae experiences a Dielectrophoresis (DEP) force i.e. $F_{DEP}$ as per *eq. (9-11)*, where, $\varepsilon_r^*$, $_p$ and $\varepsilon_{r,p}$ denotes the complex permittivity of particles and fluid in that order. ∇|E| signifies root mean square of the gradient of the square of the electric field. *CM* is known as Clausius-Mossotti factor. The radius of the particle is $r_p$ and complex permittivity of the medium is a function of electrical conductivity ($\sigma$) of the fluid and angular frequency ($\omega$) of the operation.

$$F_{DEP} = 2\pi r_p^3 \varepsilon_0 re\left(\varepsilon_r^*\right) re\left(CM\right) \nabla \left|\vec{E}\right|^2 \quad (9)$$

$$CM = \frac{\left(\varepsilon_{r,p}^* - \varepsilon_r^*\right)}{\left(\varepsilon_{r,p}^* + 2\varepsilon_r^*\right)} \quad (10)$$

$$\varepsilon_r^* = \varepsilon_r - \left(i\sigma / \omega\right) \quad (11)$$

$$F_{Tot} = F_{DEP} - F_{Drag} = m_p \frac{dv}{dt} \quad (12)$$

Finally, the *particle tracing for fluid flow (fpt)* modules gave rise to following balanced *eq.(12)* (where $F_{Tot}$ is the total or cumulative force acting on particles) that would govern the motion, direction or trajectories of the microalgae inside the liquid solution.

**Boundary condition:** In the simulation of *MPS* module, the wall of the microchannel was insulated from the surrounding environment. This setup was realized with an *electric current (ec)* module.

*Inlet A* of the microchannel was used for the flow of medium carrying microalgae while the i*nlet B* was used for buffer solution that could be used to increase or decrease the velocity and nature of flow of microalgae (**Figure 1**). These microalgae were let to pass through the top and bottom electrodes (material: gold) which imparted AC-DEP voltage on them. This effect led to a gradual separation of microalgae, based on their lipid content. It meant that the microalgae with higher lipid contents exited from *outlet B* and the others departed via *outlet A*. The size, shape, and inter-electrode distance played a very crucial role in deciding the strength of gradient of the square of the electric field in between the top and bottom electrodes, which in turn, impact the overall DEP force in the microchannel (*eq.(4)*).

In the *laminar flow (spf)* module, the wall of the microchannel was realized as a solid structure with *No-slip* condition. The inlets are given with *normal inflow velocity* in the y-direction (**Figure 1**). In the outlet section, the suppressing of the backflow condition is realized.

In the *particle tracing for fluid flow (fpt)* module, two types of microalgae (**Table 1**) with different electrical parameters were incorporated into two distinct *particle properties* feature. Then, the setting for the wall and outlets of the channel was kept as *Bounce and freeze* respectively. The drag force and DEP force were selected as the major force acting on the microalgae. To count the microalgae in the distinct outlets, *particle counter* feature was incorporated in the outlets with respect to the desired microalgae.

In the *ETS* geometry, the electrode structure and conditions were kept the same as *MPS* for individual microchannel. However, a strip of the top and bottom electrodes would connect all the microchannel that run parallel to each other (**Figure 2**). These electrode strips were designed as 0.*1 mm wide* and *4.3 mm long.* They would exert the same electric potential as the array of top and bottom electrodes respectively.

The boundary condition in *laminar flow* and *particle tracing for fluid flow (fpt)* were kept the same as *MPS* for individual microchannel. However, in. *Heat transfer in fluids (ht)*, the microchannels were set as the *fluid object* but the rest parts (PDMS layer, Silica glass substrate and

copper base) were set as the *solid objects*. The ambient room temperature (293.15 K) was set for the inlets of the microchannel. Then, heat flux features were realized on the horizontal (top and bottom), vertical section of the setup. The electrodes on the microchannel are connected to the larger sets of the electrode that serve as the contact points (**Figure 2**) for electrical potential on the microfluidic setup. These electrodes were realized as thin layers (i.e. 150 nm thick). The top electrodes array on the microchannel is connected to the electric potential source through a liquid silver layer (**Figure 2**).

## Simulations results and discussion

The particle tracking of microalgae with applied dielectrophoresis (with drag force) was conducted with various combination of frequency (100 kHz to 10 MHz), voltage amplitude (2 $V_{pp}$ to 15 $V_{pp}$), and fluid velocity (1000 µm/s to 6000 µm/s), until the final parameters (**Table 2**) were achieved. Thereafter the geometry of the channel was optimized and different sets of electrodes pairs per array were simulated. The best results were obtained with 14 pairs of the skew-symmetric gold electrode array (each array containing 4 electrodes). Each electrode is alternately 10 µm and 20 µm wide with a spacing of 20 µm throughout its length (**Figure 1**).

**Table 2:** Physical parameters used in the simulation for the microfluidic setup containing signal generator, microfluidic pump, and microfluidic setup

| | |
|---|---|
| Voltage amplitude | 12 $V_{pp}$ |
| Frequency of AC DEP | 1.894 MHz |
| Fluid velocity | 5500 µm/s |

*Laminar flow (spf)* was simulated with *Stationary* study setting. **Figure 3** shows the flow profile of the medium containing microalgae at 5.5 mm/s or 3 µL/min. The fluid flow displays constant velocity magnitude in the microchannel resulting in a stable pressure profile.

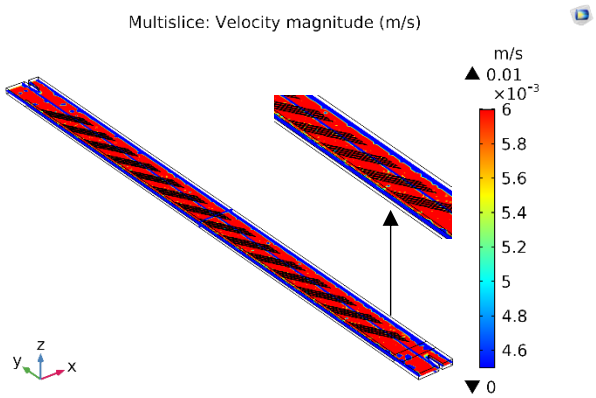


**Figure 3:** Mass flow profile of the medium containing microalgae at 5.5 mm/s or 3 µL/min from Inlet A-B towards Outlet A-B.

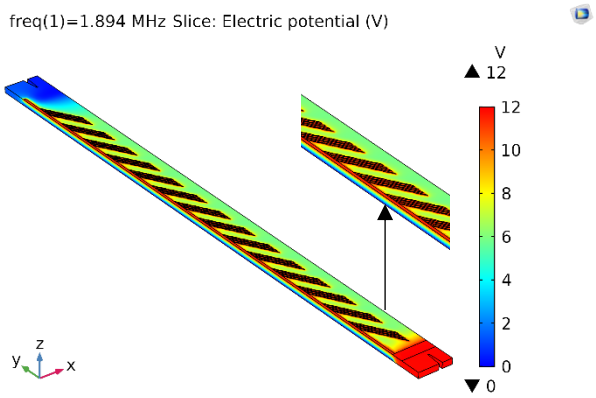


**Figure 4:** Electric potential in between top and bottom electrodes at 12 $V_{pp}$ and 1.894 MHz frequency.

Then, the *electric current (ec)* physics module was run to simulate the electric potential field in the microchannel. It was realized with *Frequency Domain* study setting at 1.894 MHz frequency. As seen in **Figure 4**, the top electrodes imparted +12V amplitude and the bottom electrodes acted as ground. Hence, the total electric potential is 12 $V_{pp}$ in the microchannel.

The gradient of the square of the electric field $\nabla\left|\vec{E}\right|^2$ simulation profile was achieved in a 3D plot group after solving for *electric current (ec)* module. The maximum value can be seen up to $10^{16}$ $V^2/m^3$ (**Figure 5**).

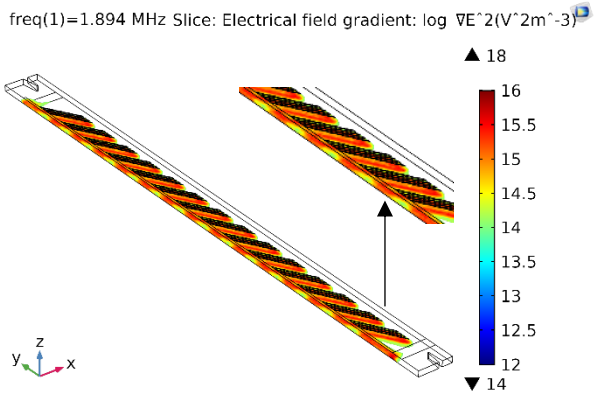


**Figure 5:** Gradient of the square of the electric field in between the top and bottom electrode. It reached up to $10^{16}$ $V^2/m^3$.

Finally, the *particle tracing of fluid flow (fpt)* was realized using a *time-dependent* study setting. This simulation was performed for 5 second time period which resulted in 100% microalgae cell separation.

***Figure 6*** illustrates that the microalgae with higher lipid content exhibited negative DEP and moved away from the electrode array and exited the microchannel via *Outlet B*. However, the other group of microalgae with less lipid content were uninfluenced by DEP force and exited via *Outlet A*. This activity made cell separation 100% efficient as mentioned in **Figure 11**.

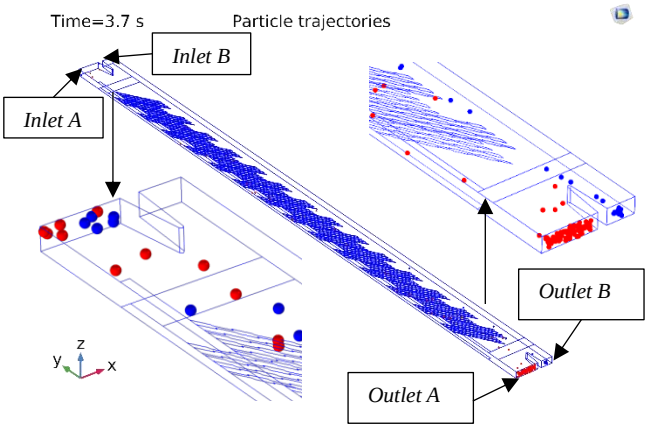


**Figure 6:** Particle trajectories of Microalgae along the y-direction from inlets A to the outlets A & B. The red microalgae have low lipid content and has an electrical conductivity of 1.2 S/m. They were not influenced by the DEP force. The blue microalgae have large lipid content with an electrical conductivity of 0.2 S/m and these microalgae were influenced by the negative DEP force. The image was taken at 3.7/5 sec of particle trajectories.

In *ETS* geometry, the temperature distribution in the setup was realized by *laminar flow (spf)* physics with *stationary* study and *electric current (ec)*, *heat transfer in fluid (ht)* physics module with frequency-*stationary* study setting. The setup was configured based on **Table 3**. Four different shapes of substrate and heat sink were inserted in the simulation using a *parametric sweep*. Then, the laminar flow and heat distribution were simulated. As seen in (**Figure 7**), temperature difference (max: 297.9 K, min: 293.15 K) was observed to be minimum in case of a substrate i.e. 300 µm thick. The maximum temperature difference (max: 300.28 K, min: 293.15 K) reached in the case of 900 µm thick substrate.

**Table 3:** Four combination of thickness for top and bottom substrate and heat sink used with parametric simulation in electro-thermal simulation. It resulted in four different temperature difference with increasing order.

| Parametric sweep parameter 1 | Parametric sweep parameter 2 | |
|---|---|---|
| Substrate height (µm) | Heat-sink height (µm) | Max/min temp difference (K) |
| 300 | 4300 | 4.7 |
| 500 | 4500 | 5.7 |
| 700 | 4700 | 6.4 |
| 900 | 4900 | 7.1 |

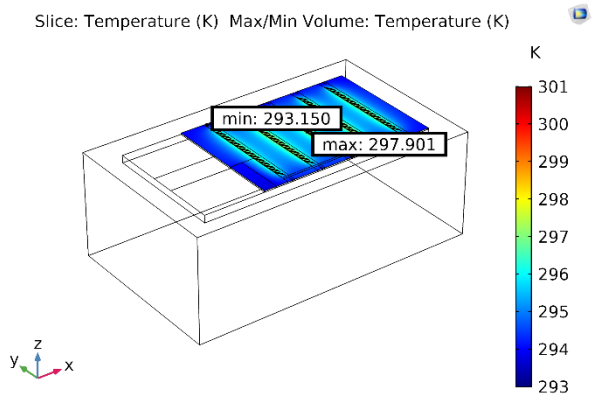


**Figure 7:** Volumetric temperature difference i.e. 4.7 K in the microfluidic system with 300 µm thick substrate and 4.3 mm thick heat sink.

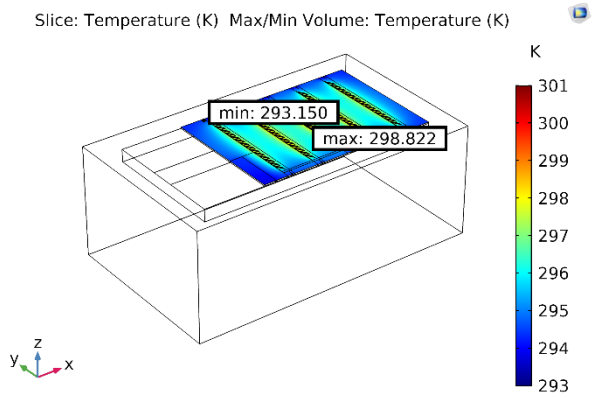


**Figure 8:** Volumetric temperature difference i.e. 5.7 K in the microfluidic system with 500µm thick substrate and 4.5 mm thick heat sink.

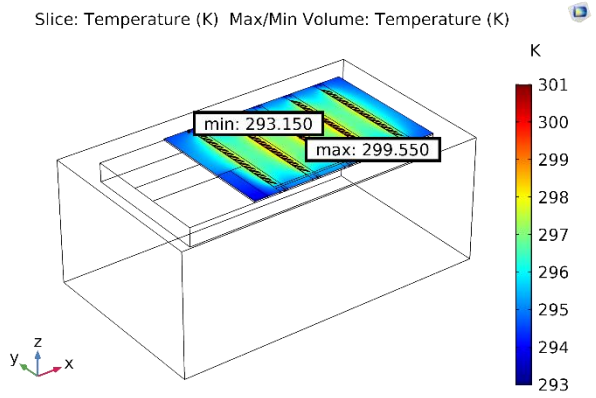


**Figure 9:** Volumetric temperature difference i.e. 6.4 K in the microfluidic system with 700µm thick substrate and 4.7 mm thick heat sink.

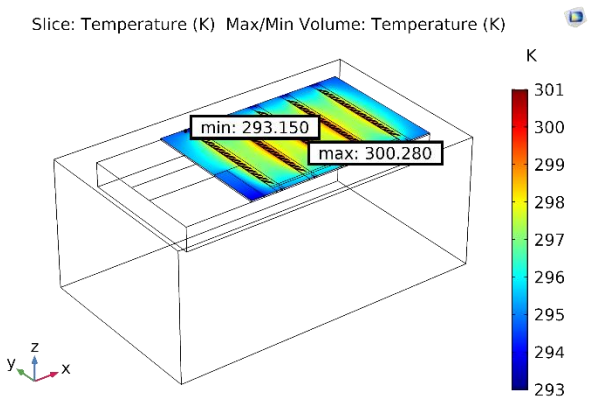


**Figure 10:** Volumetric temperature difference i.e. 7.1 K in the microfluidic system with 900µm thick substrate and 4.9 mm thick heat sink.

**Mass flow rate (µL/min) vs Cell separation:** Different fluid mass flow rate were simulated against the percentage of successful particle separation (at 12 $V_{pp}$ and 1.894 MHz). The results are seen in **Figure 11**.

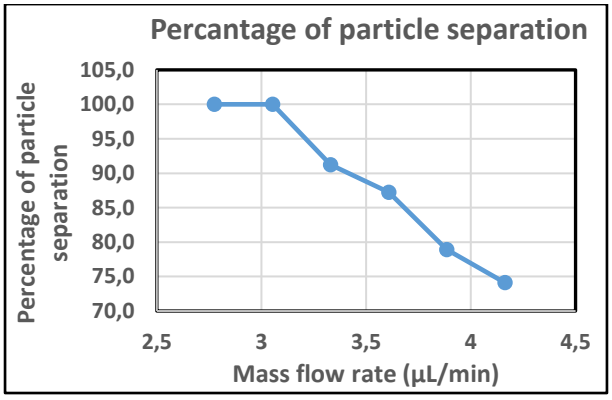


**Figure 11:** Relation between increasing mass flow rate (µL/min) and efficiency of particle separation (as percentage).

It was observed that for a high mass flow rate, microalgae separation was not efficient. However, once it reaches a value of 3 µL/min, separation becomes efficient and continue to remain so for the lower flow rate.

**Voltage amplitude vs Gradient of the square of the electric field:** As per *eq.(9-11)*, DEP force is directly proportional to the gradient of the square of the electric field i.e. $\nabla\left|\vec{E}\right|^2$. Hence, for an impactful DEP force, a strong gradient of the square of the electric field along the channel is needed. In **Figure 12**, for a visibly clear result, a microchannel with 2.5 mm length (half of the length of original microchannel used so far), 0.3 mm width and 0.05 mm height was simulated at 1.894 MHz with increasing voltage amplitude i.e. 2V to 12 V with a step increase of 2V.

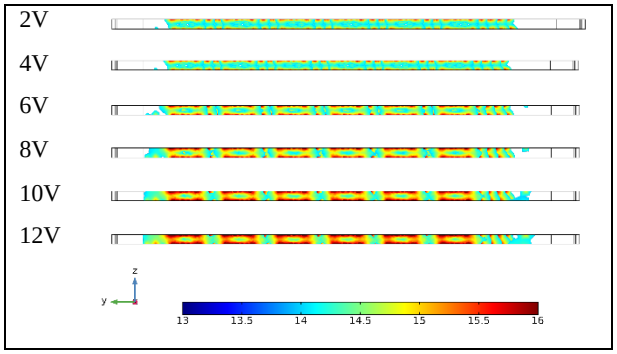


**Figure 12:** Impact of increasing voltage amplitude on the gradient of the square of the electric field i.e. $\nabla\left|\vec{E}\right|^2$.

It was observed that for an increase in the voltage amplitude, the gradient of the square of the electric field became distinctively stronger.

**The number of electrodes vs Gradient of the square of the electric field:** In order to observe the relation between the number of electrode pairs and gradient of the square of the electric field, various combinations of electrodes pairs were simulated in parametric sweep form (**Figure 13**). Initially, one electrode per array (6 arrays with 6 electrodes in total) was simulated. Then the electrode count per array increased up to two, three, and four in number i.e. 12, 18, and 24 electrodes pairs in total. As expected, the gradient of the square of the electric field and range gradually increased with the increase of electrode pairs respectively.

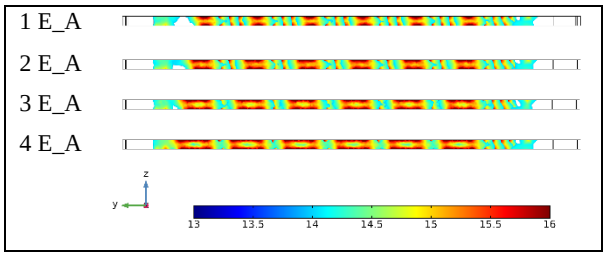


**Figure 13:** Impact of increasing electrode pairs on the gradient of the square of the electric field i.e. $\nabla\left|\vec{E}\right|^2$.

## Conclusion

For the particular case of microalgae and media investigated, it was observed that lower voltage amplitude (<12 $V_{pp}$) or lower frequency (<1.89 MHz) led to a weaker gradient of the square of the electric field in the microchannel. That resulted in the weaker DEP force acting on the microalgae. In order to create a strong DEP force, the electrodes should be skew-symmetric in shape (with zig-zag structure) and the spacing between the electrodes should be less (close to the maximum width of the skew-symmetric electrode). This structure creates a strong gradient of the square of the electric field with

the microchannel geometry. The total number of electrodes along the length of the channel is also critical to the overall DEP effect. Apart from electrode geometry, an optimum mass flow rate is important to create a smooth particle trajectory with an impactful DEP field. In this project, a maximum flow rate of up to 3 µL/min could be achieved for an efficient microalgae cell separation within one microfluidic channel.

In order to achieve high throughput inside microfluidic cell separation setup, thermal distribution, and electrical current distribution/energy loss need to be considered. The size, geometry, and material of the individual parts should also be carefully designed. In this simulation, it was observed that the temperature difference between the ambient environment and for the microalgae inside the medium is optimum for the setup with a 300 µm thick substrate and a sufficiently thick heat sink respectively.

## Acknowledgment

This work was supported by the German Federal Ministry for Education and Research (BMBF) within the funding program „Neue Produkte für die Bioökonomie“ as part of the „National research strategy bio-economy 2030“ administered by ptj Projektträger Jülich, funding number 031B0381.

## Reference

[1] M.S. Bono Jr, B.A. Ahner, B.J. Kirby, Detection of algal lipid accumulation due to nitrogen limitation via dielectric spectroscopy of Chlamydomonas reinhardtii suspensions in a coaxial transmission line sample cell, Bioresource Technology, 143 (2013) 623–631.

[2] M. Paul Abishek, J. Patel, A. Prem Rajan, Algae Oil: A Sustainable Renewable Fuel of Future, Biotechnology Research, Int. 2014 (2014) 1–8.

[3] R.R. Pethig, Dielectrophoresis: Theory, methodology and biological applications, John Wiley & Sons, 2017.

[4] H.S. Kim, T.P. Devarenne, A. Han, Microfluidic systems for microalgal biotechnology: a review, Algal Research, 30 (2018) 149–161.

[5] S.-I. Han, H.S. Kim, A. Han, In-droplet cell concentration using dielectrophoresis, Biosensors and Bioelectronics, 97 (2017) 41–45.

[6] H.A. Pohl, K. Kaler, Continuous dielectrophoretic separation of cell mixtures, Cell biophysics 1 (1979) 15-28.

[7] H.M. Ettehad, S. Guha, C. Wenger, Simulation of CMOS compatible sensor structures for dielectrophoretic biomolecule immobilization, COMSOL Conference, Rotterdam, Netherlands, 2017.

[8] G.H. Markx, R. Pethig, Dielectrophoretic separation of cells: Continuous separation, Biotechnology and Bioengineering, 45 (1995) 337–343.

[9] F. Gringel, V. Abt, P. Neubauer, M. Birkholz, Numerical analysis of dielectrophoresis for separation of microalgae, DPG-Frühjahrstagung, Berlin, 2018.

[10] A. Barai, J. Flügge, A. Hutari, P. Neubauer, M. Birkholz, Dielektrophorese-basiertes Lab-on-Chip-System zur Separation von Mikroalgen, Abstract, VDE MST Kongress, Berlin, 2019.

[11] N. Piacentini, G. Mernier, R. Tornay, P. Renaud, Separation of platelets from other blood cells in continuous-flow by dielectrophoresis field-flow-fractionation, Biomicrofluidics. 5 (2011) 034122.

[12] G. Falkovich, Fluid mechanics: A short course for physicists, Cambridge University Press, 2011.